

Available online at [www.sciencedirect.com](http://www.sciencedirect.com)

SCIENCE @ DIRECT®

Carbon xxx (2006) xxx–xxx

CARBON

[www.elsevier.com/locate/carbon](http://www.elsevier.com/locate/carbon)

## Chemical and electrochemical characterization of porous carbon materials

M.J. Bleda-Martínez<sup>a</sup>, D. Lozano-Castelló<sup>a</sup>, E. Morallón<sup>b</sup>,  
D. Cazorla-Amorós<sup>a,\*</sup>, A. Linares-Solano<sup>a</sup>

<sup>a</sup> *Departamento de Química Inorgánica, Universidad de Alicante, Ap. 99, E-03080 Alicante, Spain*

<sup>b</sup> *Departamento de Química-Física, Universidad de Alicante, Ap. 99, E-03080 Alicante, Spain*

Received 17 November 2005; accepted 11 April 2006

### 10 Abstract

11 Chemical and electrochemical techniques have been used in order to assess surface functionalities of porous carbon materials. An  
12 anthracite has been chemically activated using both KOH and NaOH as activating agents. As a result, activated carbons with high  
13 micropore volume (higher than 1 cm<sup>3</sup>/g) have been obtained. These samples were oxidized with HNO<sub>3</sub> and thermally treated in N<sub>2</sub> flow  
14 at different temperatures in order to obtain porous carbon materials with different amounts of surface oxygen complexes. Thermal treat-  
15 ment in H<sub>2</sub> was also carried out. The sample treated with H<sub>2</sub> was subsequently treated in air flow at 450 °C. Thus, materials with very  
16 similar porous texture and widely different surface chemistry have been compared. The surface chemistry of the resulting materials was  
17 systematically characterized by TPD experiments and XPS measurements. Galvanostatic and voltammetric techniques were used to deep-  
18 en into the characterization of the surface oxygen complexes. The combination of both, chemical and electrochemical methods provide  
19 unique information, regarding the key role of surface chemistry in improving carbon wettability in aqueous solution and the redox pro-  
20 cesses undergone by the surface oxygen groups. Both contributions are of relevance to understand the use of porous carbons as electro-  
21 chemical capacitors.

22 © 2006 Published by Elsevier Ltd.

23 *Keywords:* Activated carbon; Chemical treatment; Temperature programmed desorption; Electrochemical properties; Surface oxygen complexes

### 25 1. Introduction

26 Many applications of carbon materials are strongly  
27 influenced by their surface chemistry. Thus, their use in  
28 catalysis (either as catalyst or support), adsorption in solu-  
29 tion or electrochemical processes are three examples in  
30 which the surface chemistry can have an important rele-  
31 vance in the materials performance [1–5]. Specially, any  
32 discussion on the electrochemical behaviour of carbon,  
33 such as its performance as double layer capacitor, which  
34 is being very much studied nowadays, should take into  
35 account the carbon electrode/electrolyte interface, where

functional groups play an important role, mainly in aque- 36  
ous medium [1,3–16]. 37

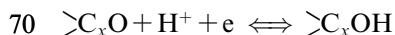
38 The presence of surface heteroatoms, especially oxygen  
39 groups, affects the electrochemical response of the carbon  
40 materials in two different ways. On one hand oxygen  
41 groups may determine the wettability by the electrolyte  
42 solution. It is known that the micropores of carbon cannot  
43 be fully wetted in aqueous solutions because of their hydro-  
44 phobic behaviour [5]. The increase in oxygen content mod-  
45 ifies the electrostatic field in the surface, imparting certain  
46 polarity, which makes easier the interaction with water  
47 molecules [1]. On the other hand, the surface oxygen  
48 groups may experience redox reactions [4,5] that can have  
49 a significant contribution to different processes.

50 An interesting example of the relevance of surface oxy-  
51 gen groups in electrochemical processes is the capacitance 51

\* Corresponding author. Fax: +34 965 903454.

E-mail address: [cazorla@ua.es](mailto:cazorla@ua.es) (D. Cazorla-Amorós).

of porous carbons, used as a component of supercapacitors. As it was shown in previous studies [5,6], the faradic current is significantly increased with the content in surface oxygen groups, while the increase in the double layer is not so important. This remarks that the enhancement in capacitance is mainly based on pseudocapacitance or redox mechanisms. Recent results showed that the promotion of capacitance with the amount of oxygen surface complexes also takes place in non-aqueous electrolyte, where wettability is not a limiting factor [7]. This idea had already been exposed by some authors [7,9–12]. Further studies in our laboratory allowed us to conclude that CO-type desorbing groups are responsible for the enhancement in capacitance [8]. The CO-type surface complexes are mainly hydroxyl, carbonyl or quinone groups which can undergo the well-known mechanism for the quinone/hydroquinone redox pair:



The role of CO<sub>2</sub>-desorbing groups is still unclear and it has been rarely reported [5]. Electron delocalization, which favours electrical conductivity is enhanced by the loss of strong electron-withdrawing groups, such as CO<sub>2</sub>-type groups [4]. In that sense, the removal of CO<sub>2</sub>-type groups should improve capacitance. This observation was previously reported [9]: the capacitance values reached a maximum after removal of the CO<sub>2</sub> groups at 450 °C. Thus, it was concluded that CO<sub>2</sub> complexes play a negative role in electrical energy storage. However this fact should be further analysed in detail.

The above comments show that to understand the electrochemical behaviour of materials, a deep characterization of the surface chemistry is necessary, which can be carried out by spectroscopic, chemical and electrochemical techniques. The characterization of surface oxygen groups is very often done by chemical or spectroscopic methods such as TPD, XPS, acid–base titration, FTIR, ... Although the measurements are, in many cases, easy, their interpretation is not simple due to the convolution of the contribution from the different functional groups. Moreover, in spite of the fact that electrochemical methods, like cyclic voltammetry, have a high surface sensitivity and the redox reactions from surface oxygen groups can be detected, it is difficult to assign the features observed to specific types of oxygen groups due to the overlapping of the different reactions and to the difficulties in the electrochemical measurements since materials with sufficient electrical conductivity should be used.

An integration of both chemical/spectroscopic methods and electrochemical techniques to deepen into the characterization of the surface chemistry could provide unique information. Unfortunately, this is not usually encountered in the literature, although there are exceptions such as Ref. [5].

Consequently, the objective of this work is to characterize activated carbons with very similar porous texture and widely different surface chemistry by chemical and electro-

chemical techniques, trying to deepen into the role of surface oxygen complexes in electrochemical properties such as the capacitance of porous carbons.

## 2. Experimental

### 2.1. Activation process

Chemical activation was done using KOH and NaOH as activating agents. An anthracite was the precursor used. Details of the preparation process are available elsewhere [17,18]. The preparation conditions for each sample are included in Table 1.

### 2.2. Chemical oxidation with HNO<sub>3</sub>

The oxidation was carried out by mixing 1.5 g of activated carbon (AK and ANa) with 20 ml of concentrated nitric acid during 3 h at room temperature. After this treatment, the samples were washed several times with hot distilled water until the pH of the filtrate was the same as the washing water. Then, the samples were dried at 100 °C. The nomenclature includes an “N” to indicate this treatment in nitric acid (i.e., samples AKN and ANaN).

### 2.3. Thermal treatments in N<sub>2</sub>

Carbons containing different amounts of surface oxygen complexes were obtained by subjecting the oxidized samples to thermal treatments at different temperatures (i.e., from 250 to 900 °C). These treatments were carried out in N<sub>2</sub> (200 ml/min) and using a heating rate of 3 °C/min. After reaching the heat-treatment temperature, it was kept for 1 h. Temperatures used are shown in Table 2. The nomenclature includes the treatment temperature (i.e., sample AKN-450 means sample AK treated in HNO<sub>3</sub> and heat-treated in N<sub>2</sub> up to 450 °C).

### 2.4. Thermal treatment in H<sub>2</sub>

One sample (CA) was thermally treated in H<sub>2</sub> flow in order to remove most of the oxygen complexes. Before thermal treatment, the sample was purified (i.e., removal of inorganic impurities) by successive treatments with aqueous solutions (10 wt.%) of HCl, HNO<sub>3</sub> and HF, respectively, at room temperature for 48 h without stirring. After HCl and HNO<sub>3</sub> treatments, the sample was repeatedly washed with deionized water up to a final pH = 4.

Table 1  
Preparation conditions in chemical activation

Sample	Activating agent	Activating agent/carbon ratio	Activation temperature (°C)	Activation time (h)	N <sub>2</sub> flow rate (ml/min)
AK	KOH	3:1	750	1	800
ANa	NaOH	3:1	750	1	800
CA	KOH	3:1	750	2	800

Table 2

Thermal treatment temperature, porous texture, quantification of oxygen surface groups in activated carbons obtained from TPD experiments and capacitance values, in all the samples studied

Sample	T (thermal treatment) (°C)	$V_{DR}(N_2)$ (cm <sup>3</sup> /g)	Average pore size DR (N <sub>2</sub> ) (nm)	$V_{DR}(CO_2)$ (cm <sup>3</sup> /g)	μmol CO/g	% CO	μmol CO <sub>2</sub> /g	% CO <sub>2</sub>	C (F/g)
AK	–	1.10	1.54	0.73	2267	80	573	20	238
AKN	–	1.05	1.72	0.68	3550	63	2059	37	254
AKN-450	450 (N <sub>2</sub> )	1.11	1.70	0.66	3333	85	573	15	232
AKN-750	750 (N <sub>2</sub> )	1.09	1.85	0.68	327	76	104	24	189
AKN-900	900 (N <sub>2</sub> )	0.98	1.67	0.61	138	55	114	45	167
ANa	–	1.06	1.69	0.70	1733	76	560	24	193
ANaN	–	1.10	1.61	0.71	2380	58	1730	42	238
ANaN-250	250 (N <sub>2</sub> )	1.09	1.64	0.69	2191	63	1312	37	242
ANaN-450	450 (N <sub>2</sub> )	1.09	1.64	0.68	2128	77	652	23	202
ANaN-750	750 (N <sub>2</sub> )	1.00	1.59	0.61	324	69	148	31	171
ANaN-900	900 (N <sub>2</sub> )	0.93	1.58	0.57	68	22	240	78	148
CA	–	1.39	1.76	0.72	2817	73	1035	27	250
CAH	850 (H <sub>2</sub> )	1.33	1.71	0.63	133	46	156	54	0.03
CAHO <sub>x</sub>	450 (air)	1.22	1.75	0.56	3708	81	889	19	191

148 After the HF treatment, it was washed with deionized  
149 water up to the final pH of the washing water and dried  
150 at 120 °C. Then, the sample was thermally treated under  
151 a hydrogen flow of 5 ml/min g at 850 °C for 3 h. This sam-  
152 ple is named as CAH. This procedure has been published in  
153 the literature [19].

#### 154 2.5. Thermal treatment in air

155 The sample CAH, previously treated in H<sub>2</sub>, was sub-  
156 jected to a thermal treatment in air flow in order to recover  
157 part of the surface oxygen groups. The process was carried  
158 out in a quartz tube fixed-bed reactor. The sample was  
159 heated at 10 °C/min up to 450 °C. Then, the temperature  
160 was kept for 12 h. This sample is named as CAHO<sub>x</sub>.

#### 161 2.6. Porous texture characterization

162 Porous texture of all samples was determined by physi-  
163 cal adsorption (N<sub>2</sub> at 77 K and CO<sub>2</sub> at 273 K) using an  
164 automatic adsorption system (Autosorb-6, Quantra-  
165 chrome) after samples out-gassing at 523 K under vacuum  
166 for 4 h. The total micropore volume (pore size below 2 nm)  
167 and the average pore size were calculated from the applica-  
168 tion of the Dubinin–Radushkevich equation to the N<sub>2</sub>  
169 adsorption at 77 K (range of relative pressures used for  
170 the DR analysis was:  $0.005 < P/P_0 < 0.17$ ). The narrow  
171 micropore volume (pore size smaller than around 0.7 nm)  
172 has been assessed from CO<sub>2</sub> adsorption at 273 K using  
173 the DR equation and for relative pressures below 0.025  
174 [20–24]. The densities of the adsorbed phases used for the  
175 calculations, were 0.808 and 1.023 g/ml for N<sub>2</sub> and CO<sub>2</sub>,  
176 respectively.

#### 177 2.7. Surface chemistry characterization

178 Temperature programmed desorption (TPD) experi-  
179 ments were done in a DSC–TGA equipment (TA Instru-  
180 ments, SDT 2960 Simultaneous) coupled to a mass

spectrometer (Thermostar, Balzers, GSD 300 T3), to char-  
181 acterize the surface chemistry of all samples. In these exper-  
182 iments, 10 mg of the sample were heated up to 950 °C  
183 (heating rate 20 °C/min) under a helium flow rate of  
184 100 ml/min.

XPS on the samples were obtained by using a VG-Mic-  
186 rotech Multilab electron spectrometer. The source  
187 employed was the MgKα (1253.6 eV) radiation of twin  
188 anode in the constant analyser energy mode. Pressure of  
189 the analysis chamber was maintained below 10<sup>−9</sup> Torr.  
190 The binding energy scale was regulated by setting the  
191 C 1s transition. Peak areas were estimated by calculating  
192 the integral of each peak after subtraction of the back-  
193 ground and fitting the experimental peak by a Gaussian  
194 curve. The binding energy values have been identified as  
195 C–C at about 284.6 eV, C–O at about 286.1 eV, C=O at  
196 about 287.3 eV and O–C=O at about 288.5 eV [25–33].  
197

#### 2.8. Electrochemical characterization

198 For the electrochemical characterization, composite  
199 electrodes were prepared from powder porous carbon  
200 material, acetylene black (Strem Chemicals) and binder  
201 (PVDC copolymer, aqueous dispersion (55% solids), Sut-  
202 ccliffe Speakman), in a ratio 77:10:13 wt.%, respectively. The  
203 materials were mixed and pressed up to 100 bars for  
204 10 min. The total electrode weight used for the measure-  
205 ments was about 70–90 mg. After that, the composite elec-  
206 trode was placed in a stainless steel mesh as a current  
207 collector. In order to measure the electric double capaci-  
208 tance of a single porous carbon electrode, the standard  
209 three electrode cell configuration was employed. Reversible  
210 hydrogen electrode (RHE) was used as reference and a  
211 platinum wire was employed as a counterelectrode. 1 M  
212 H<sub>2</sub>SO<sub>4</sub> was used as aqueous electrolyte. The galvanostatic  
213 method (at 2 mA), in a range of potentials between 0 and  
214 1 V, has been used to measure the capacitance. The capaci-  
215 tance values have been calculated from the interval  
216 between 0.2 and 0.6 V, dividing the imposed current by  
217

218 the slope of the lineal chronopotentiograms plot, taking the  
219 average value between charge and discharge processes. The  
220 result is then divided by the weight of porous carbon that is  
221 about 77% of the total composite.

222 Cyclic voltammograms have been obtained in 1 M  
223 H<sub>2</sub>SO<sub>4</sub> solution in order to assess the redox behaviour of  
224 the samples, since deviations from rectangular shape result-  
225 ing in reversible peaks indicate pseudocapacitance. The  
226 electrode and the electrochemical system employed were  
227 the same as those referred before. The scan rate was  
228 0.5 mV/s.

229 All electrochemical measurements were carried out with  
230 an EG&G Potentionstat/Galvanostat model 273 controlled  
231 by software EChem M270. All the solutions were pre-  
232 pared with ultrapure water (Purelab ELGA).

### 233 3. Results and discussion

#### 234 3.1. Porous texture characterization

235 The activated carbons prepared present type I iso-  
236 therms, what is characteristic of microporous solids.

237 Table 2 contains the micropore volumes calculated from  
238 N<sub>2</sub> adsorption data at 77 K [ $V_{DR}(N_2)$ ] and CO<sub>2</sub> adsorption  
239 data at 273 K [ $V_{DR}(CO_2)$ ] for each sample. The compari-  
240 son between the total micropore volume,  $V_{DR}(N_2)$ , and  
241 the narrow micropore volume,  $V_{DR}(CO_2)$ , gives informa-  
242 tion of the micropore size distribution [20–24]. Micropores  
243 smaller than 0.7 nm in size are measured by  $V_{DR}(CO_2)$ , and  
244 those smaller than 2 nm and bigger than 0.7 nm can be calcu-  
245 lated by the difference between  $V_{DR}(N_2)$  and  $V_{DR}(CO_2)$ .  
246 The data show that narrow micropores are 65% of the total  
247 microporosity, approximately.

248 Taking into account series AKN to AKN-900 and  
249 ANaN to ANaN-900, it can be seen that little changes in  
250 porosity occur when samples AK and ANa are oxidized  
251 and thermally treated at different temperatures. Nitric acid  
252 could either increase the porosity or block some micropo-  
253 res. According to our results, the first effect is the main  
254 one in the sample activated with NaOH, whereas the second  
255 occurs in the sample activated with KOH. The samples  
256 that have undergone the thermal treatment at higher tem-  
257 peratures present a slight decrease in micropore volume.  
258 This fact could be caused by certain structural rearrange-  
259 ment in the material [34,35]. This effect is also observed  
260 in the micropore volume reduction of sample CAH, which  
261 was strongly purified and has undergone a thermal treat-  
262 ment until 850 °C in H<sub>2</sub>.

263 We can see that these changes in porosity caused by oxi-  
264 dation and thermal treatments are very slight and hence,  
265 they will not affect the electrochemical behaviour in an  
266 important way.

#### 267 3.2. Surface chemistry characterization by TPD and XPS

268 Surface oxygen groups on carbon materials decompose  
269 upon heating producing CO and CO<sub>2</sub> at different tempera-

270 tures. It is known that CO<sub>2</sub> evolves at low temperatures as  
271 a consequence of the decomposition of the acidic groups  
272 such as carboxylic groups, anhydrides or lactones [24,36–  
273 38]. The evolution of CO occurs at higher temperatures  
274 and is originated by decomposition of basic or neutral  
275 groups such as phenols, ethers and carbonyls [24,36–38].

276 Series AKN to AKN-900 and ANaN to ANaN-900  
277 were characterized by TPD experiments. Figs. 1–4 show  
278 the TPD profiles corresponding to all samples.

279 Table 2 contains the quantification of the amount of CO  
280 and CO<sub>2</sub> desorbed in these experiments.

281 It can be observed that samples with different amounts  
282 of surface oxides have been prepared (from 68 to  
283 3550 μmol/g of CO and from 104 to 2059 μmol/g of CO<sub>2</sub>).

284 TPD experiments contain different peaks in the CO and  
285 CO<sub>2</sub> profiles, what indicates the presence of different types  
286 of surface oxygen groups. In the CO spectra, several peaks  
287 can be distinguished that come from the decomposition of

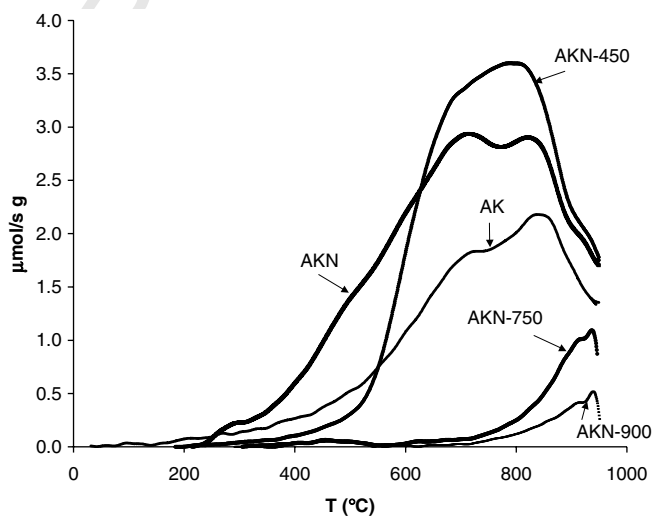


Fig. 1. TPD curves corresponding to CO desorption in AK samples.

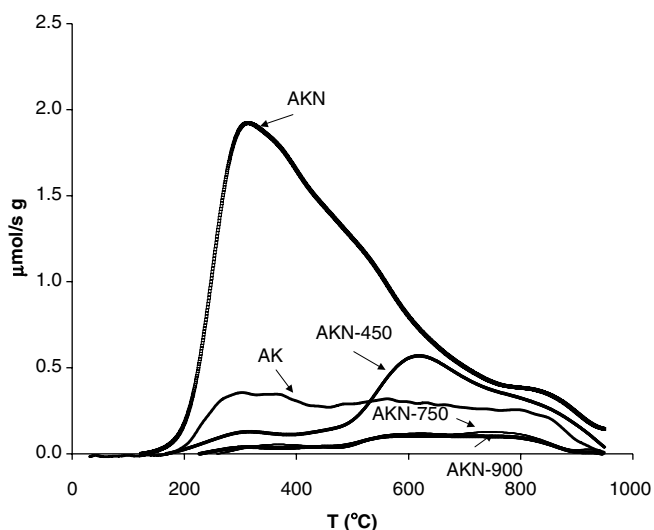


Fig. 2. TPD curves corresponding to CO<sub>2</sub> desorption in AK samples.

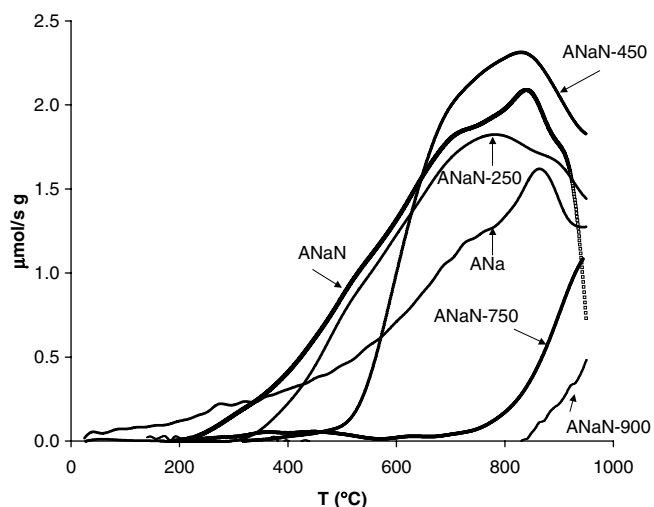


Fig. 3. TPD curves corresponding to CO desorption in ANa samples.

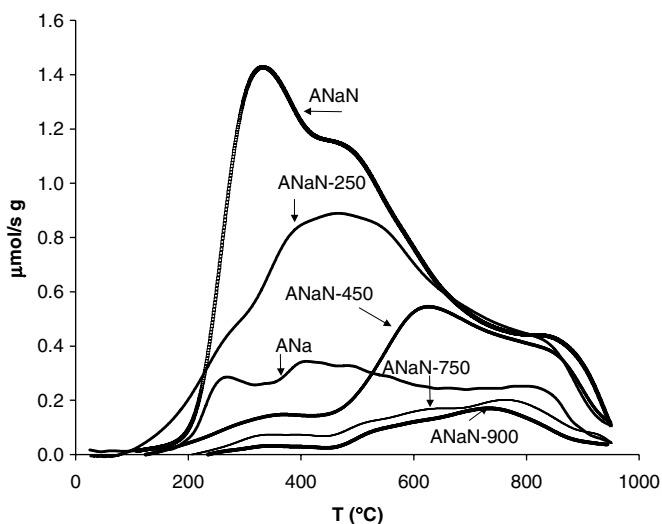


Fig. 4. TPD curves corresponding to CO<sub>2</sub> desorption in ANa sample.

288 carboxylic anhydrides (at about 500 °C) [24,37–40] and  
 289 phenol, carbonyl, quinone and ether groups (at higher tem-  
 290 peratures) [24,37–40]. In the CO<sub>2</sub> spectra, three peaks  
 291 appear. The peak at 300 °C is usually associated to car-  
 292 boxyl groups, the one at 500 °C is related to carboxylic  
 293 anhydrides and the desorption above this temperature  
 294 could be caused by lactone groups decomposition or CO<sub>2</sub>  
 295 coming from secondary reactions as these are substantially  
 296 enhanced with porous carbon [5,37–39].

297 It is known that the thermal decomposition of each car-  
 298 boxylic anhydride produces one CO molecule and one CO<sub>2</sub>  
 299 molecule at close temperatures [37–39]. In order to assess  
 300 the amount of CO and CO<sub>2</sub> associated to different func-  
 301 tional groups, the deconvolution of the CO and CO<sub>2</sub> spec-  
 302 tra was made using a multi-Gaussian function. Table 3  
 303 contains the results for the anhydride peak from the CO  
 304 and CO<sub>2</sub>-profiles deconvolution, respectively, since this  
 305 specific information will be later used.

306 As it can be observed, the CO<sub>2</sub> peak tends to appear just  
 307 a little before than CO peak. The reason why we observed  
 308 this difference is that the decomposition of carboxylic  
 309 anhydrides is not a simultaneous process. A CO<sub>2</sub> molecule  
 310 desorbs first and then the CO one. However, these desorp-  
 311 tions are very close and it is usually considered that they  
 312 take place simultaneously.

313 XPS was employed for the analysis of the surface oxy-  
 314 gen groups in the samples AKN and ANaN, since these  
 315 ones have the highest amounts of surface oxygen groups.  
 316 The distribution of oxygen complexes of each sample has  
 317 been calculated by deconvolution of the XPS spectra, fixing  
 318 the binding energy in the values presented in the experi-  
 319 mental section. The results are included in Table 4.

320 It can be observed that the percentage of O–C=O spe-  
 321 cies measured from XPS is of the same order of magnitude  
 322 (but smaller) to the percentage of CO<sub>2</sub>-type groups  
 323 obtained from the TPD experiments (Table 2). Unambigu-  
 324 ous interpretation of XPS spectra is difficult: the external  
 325 and the internal composition of a solid carbon sample  
 326 may differ and, additionally, carbon external voids can arti-  
 327 ficially lower the measured concentration of surface species  
 328 [4]. Taking into account that these two techniques are not  
 329 quantitatively comparable, we can conclude that the results  
 330 obtained by TPD and XPS are relatively consistent with  
 331 each other.

332 Samples CA, CAH and CAHO<sub>x</sub> were also subjected to  
 333 TPD experiments. The TPD profiles are shown in Figs. 5  
 334 and 6 and the quantifications are included in Table 2.

335 It is important to note the differences existing between  
 336 the samples. The main difference between sample CA and

Table 4  
 Distribution of oxygen complexes from the XPS spectra

Sample	C–O (%)	C=O (%)	CO <sub>2</sub> (%)
AKN	22	47	30
ANaN	51	19	30

Table 3  
 CO and CO<sub>2</sub> contribution to the TPD from carboxylic anhydride decomposition

Sample	CO data from anhydrides			CO <sub>2</sub> data from anhydrides		
	μmol/g	Peak temperature (°C)	Width (°C)	μmol/g	Peak temperature (°C)	Width (°C)
AKN	810	505	198	843	487	161
ANaN	525	505	198	531	433	103
ANaN-250	513	545	176	507	499	200

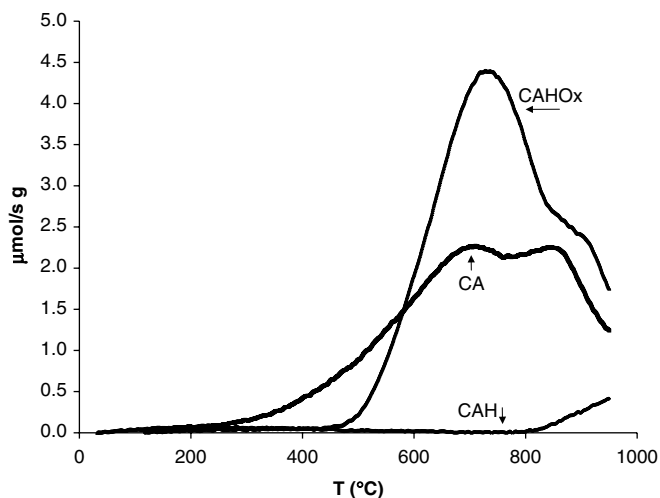


Fig. 5. TPD curves corresponding to CO desorption in CA samples.

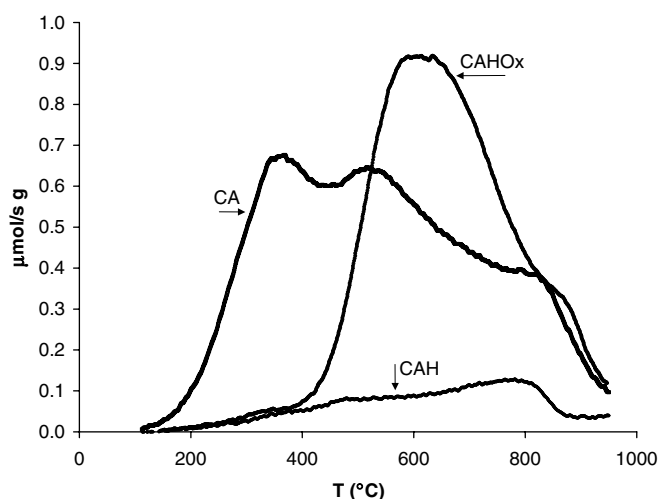


Fig. 6. TPD curves corresponding to CO<sub>2</sub> desorption in CA samples.

337 CAH is that the latter does not contain surface oxygen  
 338 groups in a significant amount. In addition, sample CAH  
 339 is different from AKN-900 and ANaN-900 from the point  
 340 of view of thermal treatment although TPD profiles are  
 341 similar: this happens because the treatment in H<sub>2</sub> has satu-  
 342 rated carbon bonds, its reactivity towards oxygen is the  
 343 lowest and it is the most hydrophobic. Then, this sample  
 344 is very useful to test the role of surface chemistry in the  
 345 wettability of the carbon material. Sample CAHO<sub>x</sub> has a  
 346 high amount of CO and CO<sub>2</sub> desorbing groups because  
 347 the treatment in air at 450 °C has generated an important  
 348 number of surface oxygen groups. However, it is important  
 349 to note that the peaks corresponding to carboxylic acids  
 350 and anhydrides do not appear in the CO<sub>2</sub> spectrum, being  
 351 the lactone peak, at temperatures above 500 °C, the only  
 352 one remaining. The CO spectrum has also changed consid-  
 353 erably since the peak at 500 °C (anhydrides) has almost  
 354 completely disappeared as expected because the heat treat-  
 355 ment temperature is very close to the temperature of anhy-  
 356 drides decomposition.

### 3.3. Electrochemical characterization: galvanostatic and voltammetric experiments

357  
 358

359 Table 2 contains the specific capacitance values for all  
 360 the samples measured for a constant current intensity of  
 361 2 mA (this corresponds to a current of about 30 mA/g).  
 362 Samples from AKN to AKN-900 and from ANaN to  
 363 ANaN-900 show that, as previously reported [8], the higher  
 364 the amount of surface oxygen groups, the higher the  
 365 capacitance.

366 Figs. 7 and 8 show the cyclic voltammograms for AKN to  
 367 AKN-900 and ANaN to ANaN-900 samples.

368 An ideal double layer capacitance behaviour of an elec-  
 369 trode material should consist of a rectangular shape of the  
 370 cyclic voltammogram. The phenomenon, then, is purely  
 371 electrostatic. On the other hand, materials with pseudoca-  
 372 pacitance show redox peaks related to electron transfer  
 373 reactions. Such redox processes can be observed in the vol-  
 374 tammograms included in Figs. 7 and 8, especially for sam-  
 375 ples AKN, AKN-450 (Fig. 7) and ANaN and ANaN-450  
 376 (Fig. 8). If the voltammograms are observed carefully, sev-  
 377 eral overlapping peaks from 0.5 to 0.65 V can be distin-  
 378 guished, being the main features an oxidation peak at  
 379 0.5 V and a second one at 0.63 V, approximately. The  
 380 reduction peaks are less defined. The existence of this  
 381 broad peak shows that different redox processes are  
 382 involved. The peak at 0.63 V is more intense for the most  
 383 oxidized samples (AKN, ANaN). In addition, it disappears  
 384 almost completely after thermal treatment at 450 °C.  
 385 Moreover, after thermal treatments at 750 °C or 900 °C,  
 386 all the peaks seem to disappear, obtaining a quasi-rectan-  
 387 gular shape in the voltammograms, indicating again that  
 388 surface oxygen groups are contributing to capacitance by  
 389 redox reactions.

390 In a previous work, an excellent correlation between  
 391 CO-desorbing groups and capacitance (both referred to  
 392 the porosity of the material) was observed [8]. The corre-  
 393 sponding plot (capacitance vs. CO-type groups) was made

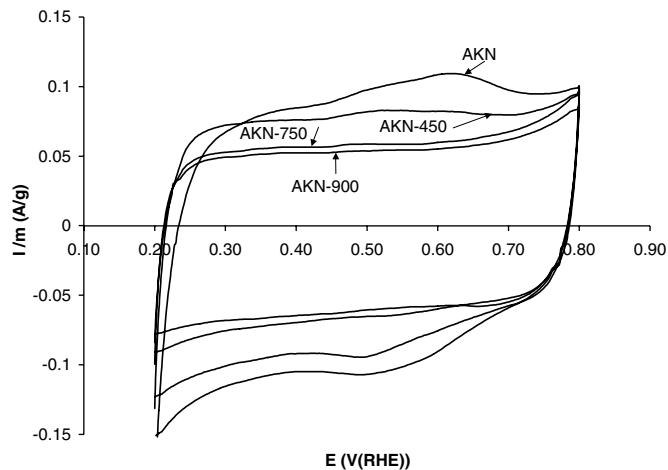


Fig. 7. Steady cyclic voltammograms of AK series. 1 M H<sub>2</sub>SO<sub>4</sub>, V = 0.5 mV/s.

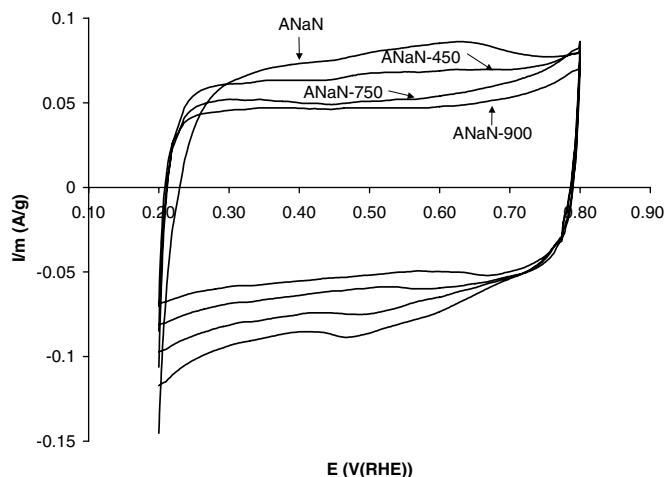


Fig. 8. Steady cyclic voltammograms of ANa series. 1 M H<sub>2</sub>SO<sub>4</sub>,  $V = 0.5$  mV/s.

394 with these series of samples (Fig. 9). Let us note that in this  
 395 case the plot has been done without dividing by the poros-  
 396 ity of the materials, due to the very similar porous texture  
 397 of these samples; however, if this parameter is taken into  
 398 account (for example, by dividing by the VDR(N<sub>2</sub>) in  
 399 Table 2), a better correlation is obtained. In any case, a  
 400 clear correlation between capacitance and the CO-type  
 401 groups exists. The samples heat-treated at 450 °C or higher  
 402 temperatures, follow a linear trend (except for sample  
 403 ANaN-900 due to its lower porosity – Table 2), but the rest  
 404 of the samples exhibit an upwards deviation. The main dif-  
 405 ference between these two groups of samples is that those  
 406 treated above 450 °C do not contain a significant amount  
 407 of carboxyl groups and anhydrides. Then, either both type  
 408 of surface oxygen groups or one of them is the responsible  
 409 for the additional contribution to the capacitance.

410 To check this point, sample ANaN-250 was obtained by  
 411 heat treatment up to 250 °C, in order to remove most of the  
 412 carboxylic groups without decomposing the anhydrides.  
 413 Interestingly, the capacitance of sample ANaN-250 is

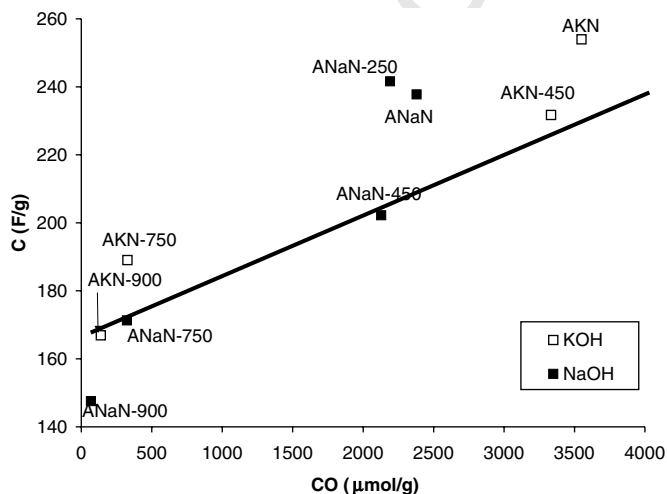
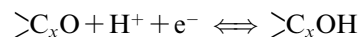


Fig. 9. Capacitance vs. CO content.

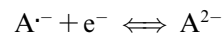
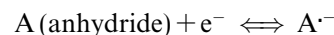
414 slightly better than that of sample ANaN. This suggests  
 415 that carboxylic groups do not play an important role in  
 416 the promotion of capacitance, although it seems that their  
 417 contribution to this property is not positive, as previously  
 418 proposed [4,9].

419 From the previous comments, it can be concluded that  
 420 carboxylic anhydrides could be the responsible for the  
 421 enhancement in capacitance, since these kinds of groups  
 422 only exist in the samples not treated above 400–550 °C,  
 423 which is the desorption temperature interval of anhydrides.

424 Taking into account that a redox peak at 0.63 V appears  
 425 in cyclic voltammograms for samples treated at lower tem-  
 426 peratures than 450 °C and that it almost disappears after  
 427 treatment at 450 °C, it can be suggested that anhydrides  
 428 undergo a redox reaction at this potential. This reaction  
 429 should be somehow different from that occurring in carbo-  
 430 nyls or quinone groups, which redox process should occur  
 431 at lower potentials. According to our experiments they are  
 432 mainly associated to the first peak in cyclic voltammo-  
 433 grams. It is known that the reduction potential of the pair  
 434 quinone/hydroquinone is located at, approximately, 0.7 V  
 435 vs. NHE. However, as it has been previously published,  
 436 an increase in the number of aromatic rings causes the for-  
 437 mal potential to decrease [5] and can reach values close to  
 438 0.5 V [1]. Taking into account that the basic structure of  
 439 activated carbons is based on graphene layers, the decrease  
 440 in the expected potential could be logical and the process  
 441 located below 0.6 V presumably proceeds through a one  
 442 electron transfer quinone/hydroquinone mechanism [4]:



445 The reaction mechanism for the oxidation/reduction of  
 446 anhydrides (at about 0.63 V) is not very clear. Many elec-  
 447 trochemistry textbooks indicate that carboxyl groups are  
 448 inactive electrochemically. However, it must be considered  
 449 that, on carbon materials, the nature of the substrate can  
 450 have a substantial effect on the electrochemical behaviour  
 451 of the available functional groups; for instance, large ara-  
 452 matic substrates and activating functional neighbours can  
 453 facilitate their reduction [4]. In organic chemistry literature,  
 454 studies related to oxidation and reduction of anhydrides in  
 455 organic medium can be found [41,42] and the following  
 456 mechanism is proposed:



461 Despite the fact that anhydrides could be hydrolysed in  
 462 aqueous medium, the thermodynamic and kinetic stability  
 463 of these functional groups can be enhanced by electron  
 464 delocalization in the  $\pi\pi$  orbitals of the graphene layers.  
 465 An experimental observation of this effect can be found  
 466 in Ref. [38]. A sample oxidized in air which contained a  
 467 large number of anhydrides was put in contact with a  
 468 wet atmosphere for a long period of time, and after drying  
 469 at low temperatures, the TPD experiment still revealed the  
 470 presence of an important amount of this type of groups.

471 Thus, the hydrolysis of these groups linked to graphene  
472 layers, seems to be slow.

473 According to the redox scheme presented above, each  
474 anhydride group will contribute with two electrons in the  
475 redox process. If we consider this aspect in the capacitance  
476 vs. CO-type groups plot presented in Fig. 9 (that is, to take  
477 into account that one anhydride contributes with two elec-  
478 trons in the redox process), we will have to change the plot  
479 for samples treated under 450 °C. Each carboxylic anhy-  
480 dride contributes to capacitance with two electrons, so  
481 the amount of anhydrides should be taken into account  
482 twice when the plot is done vs. CO. The amount of CO  
483 desorbing groups in the corrected plot, corresponds to  
484 the CO desorbed in TPD experiments plus the part corre-  
485 sponding to anhydrides (obtained from the deconvolution).  
486 Then Fig. 10 is obtained in which all the samples fit much  
487 better to the linear trend.

488 This result could indicate that anhydrides play a special  
489 role in the redox contribution of the surface oxygen com-  
490 plexes in the capacitance. In our previous work [8], we  
491 did not observe this contribution as we used the activated  
492 carbons without any treatment after activation. Because  
493 the activation temperature is usually higher than 700 °C,  
494 anhydrides groups will not remain in the carbon material.  
495 Then, to observe this effect it is necessary the selection of  
496 samples with appropriate surface chemistry as we did in  
497 this study.

498 On the other hand, CA series evidences that surface  
499 chemistry has also a key role in improving carbon wettabil-  
500 ity. As it can be observed, sample CAH, the most hydro-  
501 phobic one, presents a negligible value of capacitance  
502 (Table 2) in agreement with results obtained with graphite  
503 fibers [43]. When this sample is reoxidized in air flow, it  
504 practically recovers the capacitance value of the original  
505 sample (Table 2). The capacitance value of CAHO<sub>x</sub> sample  
506 is smaller than that of sample CA, but this can be under-  
507 stood taking into account that this sample has lost some  
508 surface area and some structural order due to the aggres-

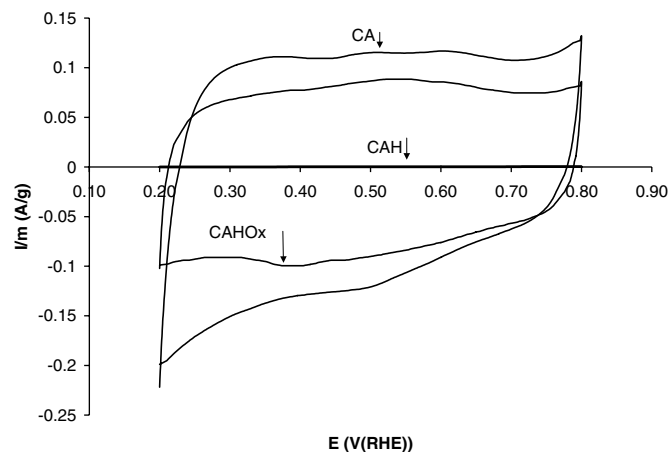


Fig. 11. Steady cyclic voltammograms of CA series. 1 M H<sub>2</sub>SO<sub>4</sub>, V = 0.5 mV/s.

509 sive procedure carried out before H<sub>2</sub> thermal treatment.  
510 Fig. 11 contains the cyclic voltammograms for samples  
511 CA, CAH and CAHO<sub>x</sub>.

512 Interestingly, we can deduce that only the heat treat-  
513 ment in hydrogen produces such a decrease in wettability,  
514 because the surface oxygen-containing samples and those  
515 heat-treated in inert atmosphere (i.e., AKN-900 and  
516 ANaN-900 samples), still have enough wettability to create  
517 most of the double layer, showing the role of dangling  
518 bonds in this property.

519 It can be observed that in CA sample a broad peak  
520 appears as it happened in the AKN and ANaN samples.  
521 However, the intensity of the peak at 0.63 V is lower  
522 because the content in carboxylic anhydrides is smaller  
523 than in the samples oxidized by HNO<sub>3</sub>. In the voltammo-  
524 gram of sample CAHO<sub>x</sub>, the redox process below 0.6 V,  
525 related to quinone/hydroquinone redox pair, has the high-  
526 est intensity. It is important to note that this sample has  
527 a low content in carboxylic anhydrides as it can be seen in the  
528 TPD spectra (Figs. 5 and 6).

529 Finally, it should be noted that the presence of surface  
530 oxides also has an influence in the formation and structure  
531 of the double layer, as a consequence of the ion–ion inter-  
532 actions between surface oxygen groups and electrolyte ions  
533 (H<sup>+</sup> and HSO<sub>4</sub><sup>-</sup> in this case). This type of interactions might  
534 have an influence on the kinetics of the charge–discharge  
535 process and on the effective pore dimensions. These ques-  
536 tions need to be studied in future work.

#### 4. Conclusions

537 Activated carbons with similar porosity but different  
538 surface chemistry have been studied by chemical and elec-  
539 trochemical methods to characterize their surface chemis-  
540 try. The combination of both techniques has allowed us  
541 to deepen into the surface electrochemical properties of  
542 porous carbon materials. Thus, the features observed in  
543 the steady cyclic voltammograms have been tentatively  
544 assigned to redox processes associated to CO-type groups  
545

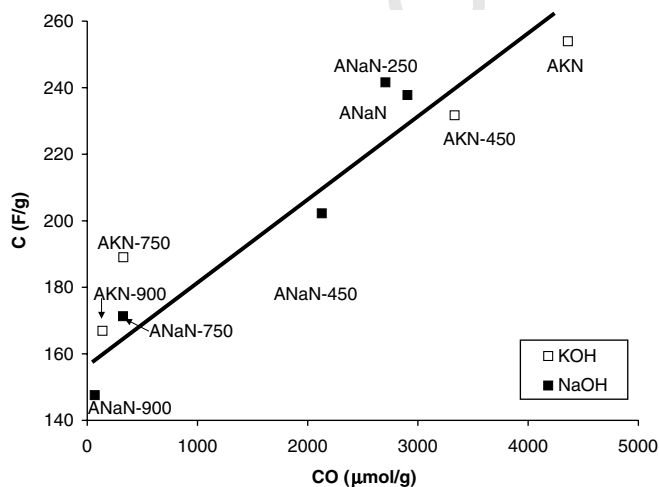


Fig. 10. Capacitance vs. CO content. Corrected values to take into account the contribution of anhydrides.



(broad peak below 0.6 V RHE) and carboxylic anhydrides (peak at about 0.63 V RHE). The surface oxygen groups have, at least, a twofold relevant contribution to the total capacitance of porous carbons. On one hand, the surface oxygen groups have an important contribution to the capacitance through faradic processes which involve one or two electron transfer reactions. On the other hand, the surface oxygen groups (or the dangling bonds created after decomposition in inert atmosphere), determine the wettability of aqueous electrolyte; thus, their presence on the carbon surface is essential to take profit of the large double layer contribution to the capacitance of the porous carbons which is associated to their high porosity. Further studies in organic medium will be done to understand the role of these functionalities in the capacitance.

### 561 Acknowledgements

562 The authors thank MEC for financial support (Project  
563 PPQ2003-03884) and I.M.J. Vilella for thermal treatment  
564 in H<sub>2</sub> carried out with sample CA. M.J.B.-M. thanks  
565 MEC for the thesis grant.

### 566 Appendix A. Supplementary data

567 N<sub>2</sub> and CO<sub>2</sub> adsorption isotherms and their DR plots  
568 are available as supplementary material on the web. Sup-  
569plementary data associated with this article can be found,  
570 in the online version, at doi:10.1016/j.carbon.2006.04.017.

### 571 References

572 [1] Kinoshita K. Carbon: electrochemical and physicochemical proper-  
573 ties. New York: John Wiley & sons; 1988, p. 293–387.  
574 [2] Radovic LR, Rodríguez-Reinoso F. Carbon materials in catalysis. In:  
575 Thrower PA, editor. Chemistry and physics of carbon, vol. 25. New  
576 York: Dekker; 1997. p. 243–358.  
577 [3] Radovic LR, Moreno-Castilla Carlos, Rivera-Utrilla J. Carbon  
578 materials as adsorbents in aqueous solutions. In: Radovic LR, editor.  
579 Chemistry and physics of carbon, vol. 27. New York: Dekker; 2001.  
580 p. 227–405.  
581 [4] Leon y Leon CA, Radovic LR. Interfacial chemistry and electro-  
582 chemistry of carbon surfaces. In: Thrower PA, editor. Chemistry and  
583 physics of carbon, vol. 24. New York: Dekker; 1994. p. 213–310.  
584 [5] Biniak S, Swiatkowski A, Pakula M. Electrochemical studies of  
585 phenomena at active carbon-electrolyte solution interfaces. In: Rado-  
586 vic LR, editor. Chemistry and physics of carbon, vol. 27. New  
587 York: Dekker; 2001. p. 125–225.  
588 [6] Hsieh C, Teng H. Influence of oxygen treatment on electric double-  
589 layer capacitance of activated carbon fabrics. Carbon 2002;40:667–74.  
590 [7] Lozano-Castelló D, Cazorla-Amorós D, Linares Solano A, Shiraishi  
591 S, Kurihara H, Oya A. Influence of pore structure and surface  
592 chemistry on electric double layer capacitance in non-aqueous  
593 electrolyte. Carbon 2003;41:1765–75.  
594 [8] Bleda-Martínez MJ, Maciá-Agulló JA, Lozano-Castelló D, Morallón  
595 E, Cazorla-Amorós D, Linares-Solano A. Role of surface chemistry  
596 on electric double layer capacitance of carbon materials. Carbon  
597 2005;43:2677–84.  
598 [9] Nian Y, Teng H. Influence of surface oxides on the impedance  
599 behaviour of carbon-based electrochemical capacitors. J Electroanal  
600 Chem 2003;540:119–27.

[10] Hu C, Wang C. Effects of electrolytes and electrochemical pretreat-  
601 ments on the capacitive characteristics of activated carbon fabrics for  
602 supercapacitors. J Power Sources 2004;125:299–308. 603  
[11] Okajima K, Ohta K, Sudoh M. Capacitance behaviour of activated  
604 carbon fibers with oxygen-plasma treatment. Electrochim Acta  
605 2005;50(11):2227–31. 606  
[12] Cheng PZ, Teng H. Electrochemical responses from surface oxides  
607 present on HNO<sub>3</sub> treated carbons. Carbon 2003;41:2057–63. 608  
[13] Li C, Wang D, Liang T, Wang X, Wu J, Hu X, et al. Oxidation of  
609 multiwalled carbon nanotubes by air: benefits for electric double layer  
610 capacitors. Powder Technol 2004;142:175–9. 611  
[14] Frackowiak E, Béguin F. Carbon materials for electrochemical  
612 storage of energy in capacitors. Carbon 2001;39:937–50. 613  
[15] Miyake M. Electrochemical functions. In: Yosuda E, Inagaki M,  
614 Kaneko K, Endo M, Oya A, Tanabe Y, editors. Carbon  
615 alloys. Amsterdam: Elsevier; 2003. p. 435–45. 616  
[16] Sullivan MG, Schnyder B, Bärtsch M, Allia D, Barbero C, Imhof  
617 R, et al. Electrochemically modified glassy carbon for capacitor  
618 electrodes. Characterization of thick anodic layers by cyclic voltam-  
619 metry, differential electrochemical mass spectrometry, spectroscopic  
620 ellipsometry, X-ray photoelectron spectroscopy, FTIR and AFM. J  
621 Electrochem Soc 2000;147(7):2636–46. 622  
[17] Lozano-Castelló D, Lillo-Ródenas MA, Cazorla-Amorós D, Linares-  
623 Solano A. Preparation of activated carbons from Spanish anthracite.  
624 I. Activation by KOH. Carbon 2001;39(5):741–9. 625  
[18] Lillo-Ródenas MA, Lozano-Castelló D, Cazorla-Amorós D, Linares-  
626 Solano A. Preparation of activated carbons from Spanish anthracite.  
627 II. Activation by NaOH. Carbon 2001;39(5):751–9. 628  
[19] Vilella IMJ, de Miguel SR, Salinas-Martínez de Lecea C, Linares-  
629 Solano A, Scelza OA. Catalytic performance in citral hydrogenation  
630 and characterization of PtSn catalysts supported on activated carbon  
631 felt and powder. Appl Catal 2005;281:247–58. 632  
[20] Rodríguez-Reinoso F, Linares-Solano A. Microporous structure of  
633 activated carbons as revealed by adsorption methods. In: Thrower  
634 PA, editor. Chemistry and physics of carbon, vol. 21. New  
635 York: Dekker; 1989. p. 1–146. 636  
[21] Cazorla-Amorós D, Alcaniz-Monge J, Linares-Solano A. Character-  
637 ization of activated carbon fibres by CO<sub>2</sub> adsorption. Langmuir  
638 1996;12(11):2820–4. 639  
[22] Cazorla-Amorós D, Alcaniz-Monge J, De la Casa-Lillo MA, Linares-  
640 Solano A. CO<sub>2</sub> as an adsorptive to characterize carbon molecular  
641 sieves and activated carbons. Langmuir 1998;14(16):4589–96. 642  
[23] Linares-Solano A, Salinas-Martínez de Lecea C, Alcaniz-Monge J,  
643 Cazorla-Amorós D. Further advances in the characterization of  
644 microporous carbons by physical adsorption of gases. Tanso  
645 1998;185:316–25. 646  
[24] Rodríguez-Reinoso F, Molina-Sabio M. Textural and chemical  
647 characterization of microporous carbons. Adv Coll Interf Sci  
648 1998;76–77:271–94. 649  
[25] Rodríguez NM, Anderson PE, Wootsch A, Wild U, Schlögl R, Paál  
650 Z. XPS, EM and catalytic studies of the accumulation of carbon on Pt  
651 black. J Catal 2001;197:365–77. 652  
[26] Pakula M, Biniak S, Swiatkowski A, Neffe S. Influence of progressive  
653 surface oxidation of nitrogen-containing carbon on its electrochemi-  
654 cal behaviour in phosphate buffer solutions. Carbon 2002;40:  
655 1873–81. 656  
[27] Kelemen SR, Freund H. XPS characterization of glassy-carbon  
657 surfaces oxidized by O<sub>2</sub> and CO<sub>2</sub> and HNO<sub>3</sub>. Energy Fuels  
658 1988;2(2):111–8. 659  
[28] Takahagi T, Ishitani A. XPS studies by use of the digital difference  
660 spectrum technique of functional groups on the surface of carbon  
661 fiber. Carbon 1982;22(1):43–6. 662  
[29] Smiley RJ, Delgass WN. AFM, SEM and XPS characterization of  
663 PAN-based carbon fibres etched in oxygen plasmas. J Mater Sci  
664 1993;28:3601–11. 665  
[30] Moreno-Castilla C, López-Ramón MV, Carrasco-Marín F. Changes  
666 in surface chemistry of activated carbon by wet oxidation. Carbon  
667 2000;38:1995–2001. 668

- 669 [31] Boehm HP. Surface oxides on carbon and their análisis: a critical  
670 assessment. Carbon 2002;40:145–9. 690
- 671 [32] Yue ZR, Jiang W, Wang L, Gardner SD, Pittman Jr CU. Surface  
672 characterization of electrochemically oxidized carbon fibers. Carbon  
673 1999;37:1785–96. 691
- 674 [33] Valdés H, Sánchez-Polo M, Rivera-Utrilla J, Zaror CA. Effect of  
675 ozone treatment on surface properties of activated carbon. Langmuir  
676 2002;18:2111–6. 692
- 677 [34] Martín-Gullón I, Marco-Lozar JP, Cazorla-Amorós D, Linares-  
678 Solano A. Analysis of the microporosity upon thermal post-treatment  
679 of H<sub>3</sub>PO<sub>4</sub> activated carbons. Extended abstracts, Carbon Conference.  
680 Oviedo: Grupo Español del Carbón; 2003. 693
- 681 [35] Lozano-Castelló D, Cazorla-Amorós D, Linares Solano A, Quinn  
682 DF. Activated carbon monoliths for methane storage: influence of  
683 binder. Carbon 2002;40:2817–25. 694
- 684 [36] Román MC, Cazorla-Amoros D, Linares-Solano A, Salinas-Martí-  
685 nez de Lecea C. TPD and TPR characterization of carbonaceous  
686 supports and Pt/C catalysts. Carbon 1993;31:895–902. 695
- 687 [37] Figueiredo JL, Pereira MFR, Freitas MMA, Órfao JJM. Modifica-  
688 tion of the surface chemistry of activated carbons. Carbon 1999;37:  
689 1379–89. 696
- [38] Linares-Solano A, Salinas-Martínez de Lecea C, Cazorla-Amorós D,  
Joly JP, Charcosset H. Nature and structure of calcium dispersed on  
carbon. Energy Fuels 1990;4:467–74. 697
- [39] Calo JM, Hall PJ. Applications of energetic distributions of oxygen  
surface complexes to carbon and char reactivity and characterization.  
In: Lahaye J, Ehrburger P, editors. Fundamental issues in control of  
carbon gasification reactivity. Dordrecht: Kluwer Academic Pub-  
lishers; 1991. p. 336–63. 698
- [40] Calo JM, Cazorla-Amorós D, Linares-Solano A, Román-Martínez  
MC, Salinas-Martínez de Lecea C. The effects of hydrogen on thermal  
desorption of oxygen surface complexes. Carbon 1997;35(4):543–54. 699
- [41] De Luca C, Giomini C, Rampazzo L. Electrochemistry of organic  
acceptor compounds: aromatic anhydrides. J Electroanal Chem  
1987;238:215–23. 700
- [42] Nagy JB, Nagy OB, Bruylants A. Charge-transfer complexes in  
organic chemistry. XI. Effect of acceptors on the properties of charge-  
transfer complexes formed by cyclic anhydrides. J Phys Chem  
1974;78(10):980–3. 701
- [43] Frysz CA, Shui XP, Chung DDL. Effect of chemisorbed oxygen on  
the electrochemical behaviour of graphite fibers. Carbon 1994;32(8):  
1499–505. 702